Supporting Online Material for 'A Tunable Two-impurity Kondo system in an atomic point contact'

Jakob Bork,[1,2] Yong-hui Zhang,[1] Lars Diekhöner,[2] László Borda,[3,4]
Pascal Simon,[5] Johann Kroha,[3] Peter Wahl,[1] and Klaus Kern[1,6]

[1]*Max-Planck-Institut für Festkörperforschung,*
Heisenbergstrasse 1, D-70569 Stuttgart, Germany
[2]*Institut for Fysik og Nanoteknologi and Interdisciplinary Nanoscience Center (iNANO),*
Aalborg Universitet, Skjernvej 4A, DK-9220 Aalborg, Denmark
[3]*Physikalisches Institut, Universität Bonn,*
Nussallee 12, D-53115 Bonn, Germany
[4]*Department of Theoretical Physics,*
Budapest University of Technology and Economics, H-1111 Budapest, Hungary
[5]*Laboratoire de Physique des Solides, Université Paris-Sud,*
CNRS, UMR 8502, F-91405 Orsay Cedex, France
[6]*Institut de Physique de la Matière Condensée,*
Ecole Polytechnique Fédérale de Lausanne (EPFL), CH-1015 Lausanne, Switzerland

(Dated: March 30, 2011)

S1. SAMPLE PREPARATION

Experiments have been performed on a Au(111) single crystal prepared in ultra high vacuum (UHV) by cycles of sputtering and annealing to 800K. Cleanliness of the sample has been checked by scanning tunneling microscopy (STM) after transferring the crystal into the cryostat. Cobalt atoms have been evaporated onto the gold surface in-situ from a tungsten filament with a cobalt wire wound around it. Measurements have been performed in a home-built low temperature UHV-STM which operates at temperatures down to 6K. Tunneling and point contact spectra have been acquired with open feedback loop recording the $\mathrm{d}I/\mathrm{d}V$ signal from a lock-in amplifier. For the experiments shown, we used lock-in modulations in the range of $1.43 - 2.15\mathrm{mV_{RMS}}$. We have used a tungsten tip, which is cleaned by field emission and by bringing it in contact with the Au(111) surface prior to the experiments described above. A tip is judged to be good if it exhibits a sufficiently flat tunneling spectrum (apart from the onset of the surface state of Au(111) at -460mV and a linear background) and images atoms on the surface as spherical protrusions.

S2. NRG CALCULATIONS

To compute the local T-matrix containing many body effects we have chosen Wilson's numerical renormalization group (NRG) technique(*S1*, *S2*). The cornerstone of the method is the logarithmic discretization of the conduction electron band and mapping the system onto a semi-infinite chain with the impurity at the end. NRG has been successfully applied to the problem of two magnetic impurities but only thermodynamic quantities were computed(*S3*, *S4*). The main source of complication in a two-impurity calculation as compared to a single impurity case is that the former is an effectively two band calculation: From the NRG point of view it is a challenging task because the impurities now couple to two semi-infinite chains. Consequently, the Hilbert space grows by a factor 16 in each NRG step. This is still manageable with today's computer resources. Concerning the details of the present NRG calculation, we have chosen discretization parameter $\Lambda = 2$, the number of iterations was $N = 50$ and we kept $M = 4096$ states per iteration exploiting the charge and spin z-component $U(1)$ symmetries.

In figure 3C in the manuscript, only one diagonal element of the T-matrix is plotted, as

the two diagonal elements are (due to symmetry) identical in the calculation. The diagonal elements are proportional to the local density of states (LDOS) at the impurity sites.

S3. MEASUREMENT PROCEDURE FOR SPECTROSCOPY

The spectra shown in the main article are acquired in pairs. After moving the tip on top of a cobalt atom, the tip-sample distance is reduced by a predefined distance d and after a few seconds of pause to get clear of piezo creep, the first spectrum is acquired. After another few seconds of pause to assess the resulting drift during acquisition of the spectrum, the tip is approached by a small distance Δd to the next position and a repeated pause/acquisition/pause sequence is performed before the tip is returned to tunneling conditions. A topography scan is then performed to confirm that the Cobalt atoms (on the surface and on the tip) are at the same positions as before. If they are in the same positions and have preserved their shapes, the next pair of spectra are acquired. This ensures reversibility and reproducibility of the entire process, we can go in and out of contact and obtain the features repeatedly.

There is a considerable amount of piezo creep in the tip-sample distance when approaching the tip by more than 3 Å (compared to the picometer precision of the experiment). The uncertainty resulting from the creep is avoided by measuring the current during the pauses before and after acquisition of the spectra. The stable current just before acquisition of each spectrum is used as a measure for the tip-sample distance by converting the current to a value for z through a measured approach curve as shown in fig. 3A. Close to point contact, the conductance trace becomes unstable due to mechanical instabilities and due to the large slope of the conductance as a function of distance close to contact making measurements in this regime extremely sensitive to external perturbations. In point contact, the conductance trace becomes stable again, see fig. 3B.

S4. DATA FITTING

A. Tunneling and Transport Spectra

In the tunneling regime, one single Fano function(*S5–S8*) has been fitted to the spectra. In addition to the Fano function,

$$f(\omega, q) = \frac{(\omega + q)^2}{\omega^2 + 1}, \tag{S1}$$

a constant and a linear background term are taken into account

$$g(\epsilon) = af(\frac{\epsilon - \epsilon_0}{\Gamma}, q) + b\epsilon + c. \tag{S2}$$

Thus six parameters are extracted from the fits, which are the amplitude a of the resonance, its position ϵ_0, width Γ, a line-shape parameter q and two parameters b, c for the background. Depending on q, this function describes a dip for $q \sim 0$, an asymmetric resonance for $q \sim 1$ or a lorentzian peak for $q \to \infty$.

When the resonance splits, we fit the spectra with a sum of two Fano line shapes (*S9*)

$$g(\epsilon) = a_1 f(\frac{\epsilon - \epsilon_{01}}{\Gamma_1}, q_1) + a_2 f(\frac{\epsilon + \epsilon_{02}}{\Gamma_2}, q_2) + c. \tag{S3}$$

The splitting of the resonances is a direct measure for the exchange coupling I, where $I = \epsilon_{01} + \epsilon_{02}$. The error bars given are obtained from the 1σ confidence interval as obtained from the fit. In fig. S1, the fits for the spectra shown in the main text are displayed.

B. Influence of Single Impurity Line shape on apparent resonance width

As discussed in the main text, tip and sample Kondo resonance are superimposed in the tunneling spectrum. In order to explore the influence of changes in parameters of the single impurity Kondo resonances on the overall spectrum, we have simulated dI/dV-characteristics for specific sets of parameters of the single impurity resonances. Especially, as the transport characteristics through the two cobalt atoms show a transition from a dip to a peak, we have assumed that the line shape parameter q of the two impurities changes from a dip to a peak when approaching them towards each other. We find that this change of the single impurity Kondo resonance line shape can account for an apparent reduction of the overall width of the combined resonance. To model the spectra, we have assumed all parameters except the

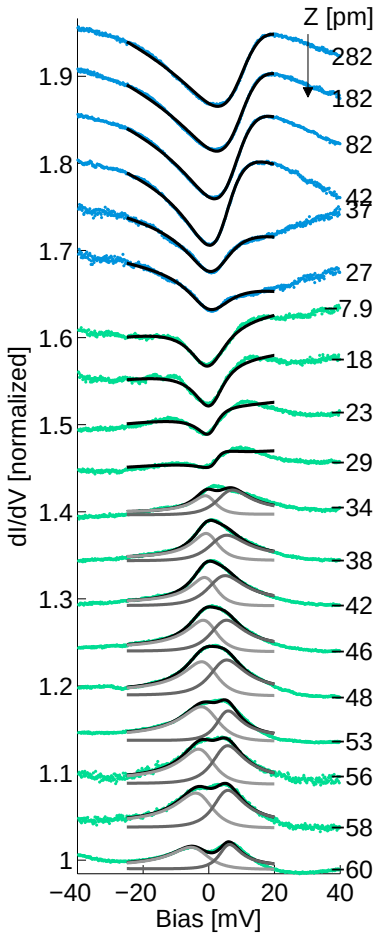

FIG. S1: Fits of eq. S2 for $z \geq -29$pm and eq. S3 for $z \leq -34$pm to the data shown in the main text in fig. 3B.

line shape parameter q to stay the same for the different tip-sample distances. For the line shape parameter q, we will assume a continuous increase on approaching the tip towards the sample as proposed for a direct tunneling channel between the two d-orbitals (this is discussed for a direct channel between the conduction band of the tip and a d-orbital of the magnetic adatom e.g. in Ref. *S10*). The resulting set of curves is shown in fig. 4C. The overall curve stays symmetric exposing a dip as long as the single impurity line shape $q < 1$. Around $q \sim 1$, the observed curve has a transition from a dip to a peak, similar to what we observe experimentally. The width of the resonance as determined from a fit of a single Fano line shape to the calculated spectra (see fig. 4A) exhibits a reduction in agreement with

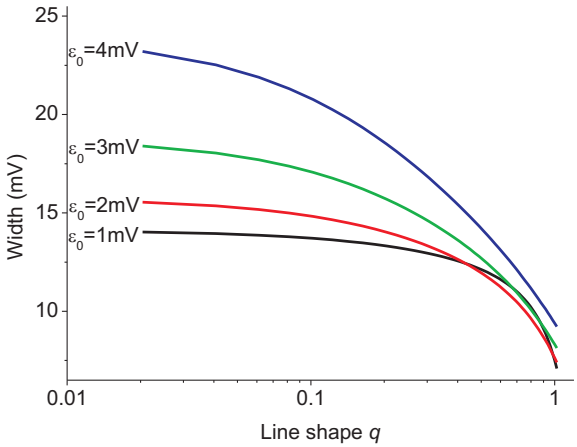

FIG. S2: Suppression of the width of the overall resonance obtained by fitting a single Fano resonance to the calculated spectra for different positions of the single impurity resonances ϵ_0. The behaviour of the width can be compared to the data shown in fig. 4C.

what we find in the experiment. It should however be noted that the calculation described above neglects any correlation or interaction effects. Although for calculating spectra, we compute the convolution, the result is basically the sum of the two Fano resonances with only minor corrections(*S11*).

The calculation is done using the expression for the tunneling current by Lang(*S12*) in the low bias limit neglecting the energy dependence of the matrix element. For the tip and sample LDOS we insert Fano line shapes (eq. S2) and assume a temperature broadening of 6K. Differential conductance is calculated taking into account a Lock-in modulation of $2\mathrm{mV_{RMS}}$. Parameters for the Fano line shapes of tip and sample are $T_\mathrm{K} = 76\mathrm{K}$, $a = 0.05$, $b = 0$, $c = 1$. To relate the line shape parameter q to the tip-sample distance, we use the relation $q = e^{-(z-z_0)/\kappa_\mathrm{d}}$. Thus to compare the width extracted from the calculation to the experiment, we adjust three parameters: the position of the resonance ϵ_0, and κ_d and z_0. From the fit, we obtain $\epsilon_0 = 3.45\mathrm{mV}$ (comparable to what is found in Ref. (*S6*)), $\kappa_\mathrm{d} = 0.45\text{Å}$.

C. Comparison to NRG calculation

To allow for a comparison of the splitting extracted from the NRG calculations with the experimental values as shown in fig. 4D, the coupling Δ, which is the input parameter of the NRG calculation corresponding to the tip-sample distance z has to be converted to a distance scale. To this end, we assume $z \propto \log \Delta + z_0$.
The antiferromagnetic coupling I obtained from the NRG calculation can be estimated to be

$$I = V_{\mathrm{s}} V_{\mathrm{t}} \rho_{\mathrm{s}} \left(E_{\mathrm{F}}\right) \rho_{\mathrm{t}} \left(E_{\mathrm{F}}\right) \Delta.$$

As from the NRG calculation basically $I \propto \Delta$, a simplistic model for the distance dependence of the exchange interaction is $I \propto e^{-(z-z_0)/\kappa_I}$. With these assumptions, we obtain $\kappa_I = (0.25 \pm 0.08)$Å (error bar from fit for 95% confidence interval).

S5. CONDUCTANCE OF COBALT-COBALT, COBALT-GOLD AND GOLD-GOLD JUNCTIONS

The conductance of single atoms can be extracted from approach curves, where the tip is positioned vertically on top of an adatom and then the current is recorded while approaching the tip towards the adatom. The clean tip is typically assumed to be terminated by a substrate atom, i.e. for a gold substrate by a gold atom. In fig. S3 we show approach curves for a junction consisting of a gold tip and a gold atom on the surface (Au-Au), a gold tip and a cobalt atom (Co-Au) and two cobalt atoms (Co-Co), the latter one being shown also in the main text. We find a significantly larger conductance of the Co-Co junction at the transition to point contact compared to Au-Au and Au-Co junctions.

S6. EXPERIMENTS WITH ONE OR NO COBALT ATOM BETWEEN TIP AND SAMPLE

As reference we have acquired spectra taken with a clean tip (tip softly indented in the Au(111) surface) on top of a gold adatom on the surface shown in fig. S4A and on top of a cobalt atom on the surface shown in fig. S4B.

The spectra acquired on top of a gold atom on the surface do not reveal any significant

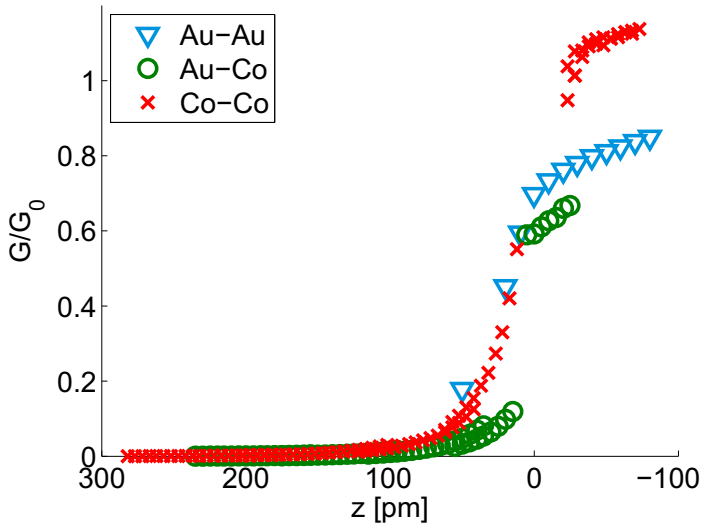

FIG. S3: Approach curves for junctions between two cobalt atoms (Co-Co), a gold tip and a cobalt atom (Au-Co), and a gold tip and a gold atom (Au-Au). Note the comparatively large conductance of the Co-Co junction.

changes in the spectroscopic features on approaching the tip from tunneling to point contact. Especially, the features seen in tunneling do not change their position nor their width in a systematic way.

In case of a cobalt adatom on the surface and a clean gold tip, the Kondo resonance can be seen until the tip jumps into point contact, where the resonance disappears and is replaced with a broad feature that is constant as a function of tip-sample distance (two lowest green curves in fig. S4B). The Kondo temperature increases slightly by $\sim$ 17K from the tunneling setpoint until the tip jumps to contact. The behaviour is somewhat different compared to what has been found for cobalt atoms on Ag or Cu single crystals (*S13*, *S14*). These experiments have shown the modification of the Kondo resonance of the cobalt atom by the presence of the tip as well as due to the influence of relaxations of the tip-adatom-surface geometry.

S7. STATISTICS

As pointed out in the main text of the paper, tip spectra after pick-up of a cobalt atom vary. Fig. S5 shows tips judged good and those discarded after pick-up of a cobalt atom, for

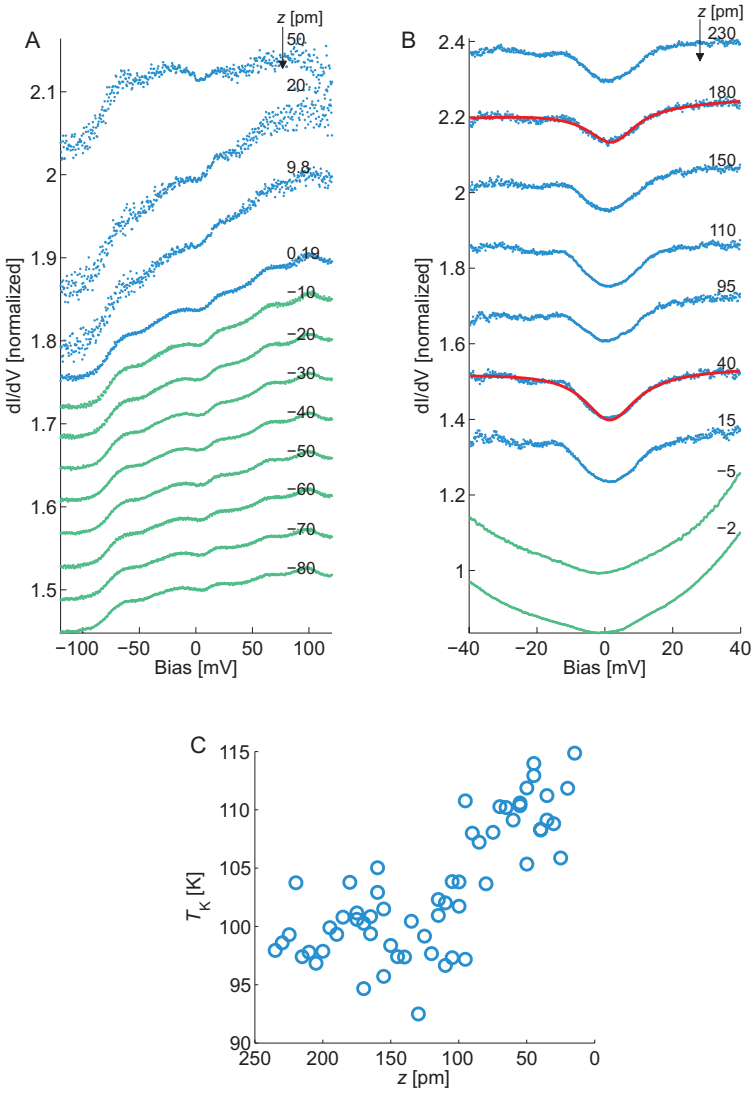

FIG. S4: Transport measurements with a clean tip (presumably with a gold atom at the apex of the tip) while approaching (**A**) a gold atom on the surface and (**B**) a single cobalt adatom on the Au(111) surface. Blue is tunneling and green is point contact. Gold atoms are deposited following the recipe discussed in Ref. *S15*. (**C**) The Kondo temperature corresponding to the resonances in B in tunneling. The spectra in B are only 1 out of every 10th spectrum taken and used in C. Spectra in A have been acquired one at a time, those shown in B in one sequence.

tip spectra taken on the clean Au(111) surface. For tips judged good (shown in fig. S5(A)), the parameters resulting from fitting a Fano function are shown in table S1. Data shown in the main text have been acquired with tip #1 (figures 3C (spectra from 300pm to 42pm)

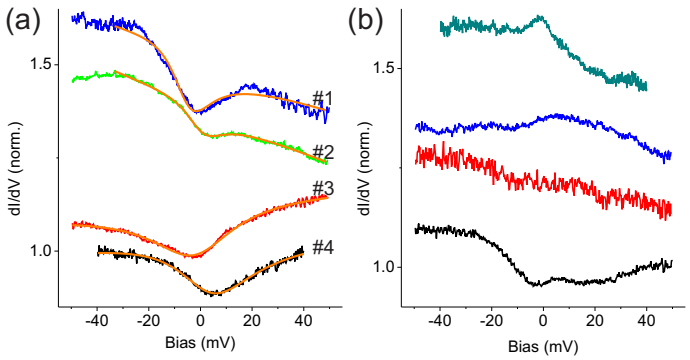

FIG. S5: Spectra taken on the clean Au(111) surface after pick-up of cobalt atom, where the cobalt atom has disappeared from the surface. A Spectra for pick-ups considered successful in the sense that spectra reveal a Kondo resonance similar to that of a cobalt atom on the surface. Solid lines show fits of a Fano function (eq. S2), the parameters are given in table S1. B Spectra after pick-ups considered unsuccessful.

Tip #	a	b	c [mV^{-1}]	Γ [mV]	ϵ_0 [mV]	q
1	0.14	0.98	-0.002	9.19	-5.44	-0.32
2	0.067	1.06	-0.003	8.79	0.09	-0.24
3	0.134	0.86	0.0006	19.4	-1.60	0.1
4	0.133	0.88	0.0005	17.6	3.25	-0.19

TABLE S1: Parameters of a Fano fit to the tip spectra shown in fig. S5. Order of appearance is the same as in the plot. Spectra have been fitted in the full range shown in fig. S5, except for tip #2 where the range was $[-30\text{mV} : 50\text{mV}]$ to exclude the downturn seen in the spectrum at the negative bias end.

and 4A (circles)) and #4 (figures 2F&G, 3C (spectra for $z \leq 37$pm) and 4A, B (triangles)), data shown in fig. S6 with tip #3.

S1. K.G. Wilson. The renormalization group: Critical phenomena and the kondo problem. *Rev. Mod. Phys.*, 47:773–840, 1975.

S2. R. Bulla, T.A. Costi, and T. Pruschke. Numerical renormalization group method for quantum

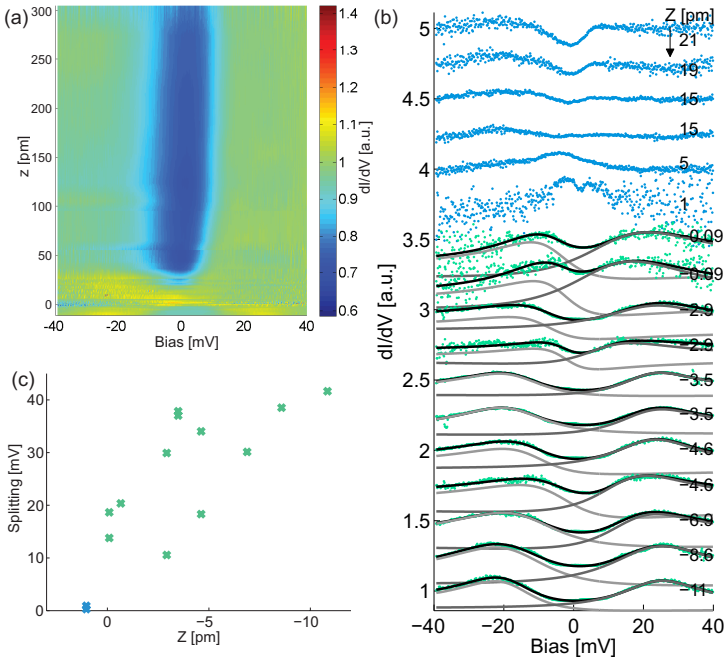

FIG. S6: Data set similar to the one shown in fig. 3 of the manuscript, obtained in an independent preparation. A spectra in the tunneling regime (color encodes conductance), B spectra around and in the point contact regime, C splitting as a function of distance, similar to fig. 4A.

impurity systems. *Rev. Mod. Phys.*, 80:395–450, 2008.

S3. B.A. Jones and C.M. Varma. Study of two magnetic impurities in a fermi gas. *Phys. Rev. Lett.*, 58:843–846, 1987.

S4. B.A. Jones, C.M. Varma, and J.W. Wilkins. Low-temperature properties of the two-impurity kondo hamiltonian. *Phys. Rev. Lett.*, 61:125–128, 1988.

S5. U. Fano. Effects of configuration interaction on intensities and phase shifts. *Physical Review*, 124(6):1866–1878, 1961.

S6. V. Madhavan, W. Chen, T. Jamneala, M.F. Crommie, and N.S. Wingreen. Tunneling into a single magnetic atom: Spectroscopic evidence of the kondo resonance. *Science*, 280:567, 1998.

S7. J. Li, W.-D. Schneider, R. Berndt, and B. Delley. Kondo scattering observed at a single magnetic impurity. *Phys. Rev. Lett.*, 80:2893–2897, 1998.

S8. O. Ujsaghy, J. Kroha, L. Szungyogh, and A. Zawadowski. Theory of the fano resonance in the

stm tunneling density of states due to a single kondo impurity. *Phys. Rev. Lett.*, 85:2557–2561, 2000.

S9. P. Wahl, P. Simon, L. Diekhöner, V.S. Stepanyuk, P. Bruno, M.A. Schneider, and K. Kern. Exchange interaction between single magnetic adatoms. *Phys. Rev. Lett.*, 98:056601, 2007.

S10. M. Plihal and J.W. Gadzuk. Nonequilibrium theory of scanning tunneling spectroscopy via adsorbate resonances: Nonmagnetic and kondo impurities. *Phys. Rev. B*, 63:085404, 2001.

S11. P. Wahl, L. Diekhöner, M.A. Schneider, and K. Kern. Background removal in scanning tunneling spectroscopy of single atoms and molecules on metal surfaces. *Rev. Sci. Instr.*, 79:043104, 2008.

S12. N.D. Lang. Spectroscopy of single atoms in the scanning tunneling microscope. *Phys. Rev. B*, 34:5947–5950, 1986.

S13. N. Néel, J. Kröger, L. Limot, K. Palotas, W.A. Hofer, and R. Berndt. Conductance and kondo effect in a controlled single-atom contact. *Phys. Rev. Lett.*, 98:016801, 2007.

S14. L. Vitali, R. Ohmann, S. Stepanow, P. Gambardella, K. Tao, R. Huang, V.S. Stepanyuk, P. Bruno, and K. Kern. Kondo effect in single atom contacts: The importance of the atomic geometry. *Phys. Rev. Lett.*, 101:216802, 2008.

S15. L. Limot, J. Kröger, R. Berndt, A. Garcia-Lekue, and W.A. Hofer. Atom transfer and single-adatom contacts. *Phys. Rev. Lett.*, 94:126102, 2005.